LOI: Next Generation Tritium Experiments in CLAS12

D. Gaskell (Spokesperson),
D.W. Higinbotham (Spokesperson), D. Meekins (Spokesperson)
Thomas Jefferson National Accelerator Facility,
Newport News, Virginia 23606, USA

A. Ashkenazi, A. Denniston, R. Cruz-Torres, O. Hen (Spokesperson)*, D. Nguyen,
A. Papadopoulou, J. Pybus, A. Schmidt, E.P. Segarra
Massachusetts Institute of Technology, Cambridge, Massachusetts 02139, USA

D. Dutta (Spokesperson),
Mississippi State University, Mississippi State, Mississippi 29762, USA

Z. Ye (Spokesperson),
Argonne National Lab, Lemont, IL 60439

F. Hauenstein, M. Khachatryan, and L.B. Weinstein (Spokesperson)
Old Dominion University, Norfolk, Virginia 23529, USA

E. Piasetzky
Tel-Aviv University, Tel Aviv 69978, Israel

S. Sirca (Spokesperson), and M. Mihovilovic (Spokesperson)
University of Ljubljana and Jozef Stefan Institute, 1000 Ljubljana, Slovenia

T. Kolar
Jozef Stefan Institute, 1000 Ljubljana, Slovenia

Abstract

This LOI includes information on possible experiments for an experimental program using a new tritium target in CLAS12. It includes several pieces, including flavor-tagged DIS on d, ^{3}He, and ^{3}H targets, and quasielastic scattering. A preliminary feasibility study indicates that a tritium target in Hall B is possible. We are submitting this LOI to get feedback from the PAC whether it is worth the effort of developing a full proposal, including significantly more work on the possible Hall B tritium target.

The bulk of the LOI discusses the flavor-tagged DIS measurement.

*Contact Person: hen@mit.edu

1 Flavor-tagged Deep Inelastic Scattering

We propose to measure precision ratios of charged pion electroproduction in Semi Inclusive Deep Inelastic Scattering from deuterium and ^{3}He and ^{3}H targets in order to test the flavor dependence of the EMC effect in the valence region. These targets are chosen to minimize hadron attenuation effects, while maximizing nuclear asymmetry.

This experiment will use the CLAS12 detector to detect the scattered electrons and knocked out pions. It will use the standard CLAS12 liquid target for deuterium and ^{3}He and a new, dedicated tritium target. The experiment will measure the semi-inclusive production of charged pions over a wide x-range, focussing on $0.2 \leq x \leq 0.6$ where valence quarks dominate. It will also focus on $z = E_\pi/\nu \geq 0.4$ to maximize the connection between the struck quark and the detected $\pi^\pm$.

We will form double ratios of the yields and ratios of the yield differences to search for evidence of flavor dependence of the EMC effect. Our simulations show that these two variables are most sensitive to flavor dependence of the EMC effect. Evidence of a flavor dependence in the EMC effect will place strict constraints on models of the EMC effect and give us new information regarding the effect of the nuclear environment on quarks. This experiment will also have impact on calculations or experiments that rely on knowledge of nuclear parton distributions at large x.

In addition, the large acceptance and PID of CLAS will also let us measure flavor tagged DIS scattering with kaons, identifying the kaons in the CLAS12 RICH detector.

This proposal builds on PR12-09-004, which had proposed to look at the ratio of gold to deuterium, but was judged to have too many nuclear uncertainties. By changing to ratios of light nuclei, we maintain the sensitivity to the underlying physics but dramatically decrease the nuclear uncertainties due to attenuation and hadronization in heavy nuclei.

1.1 Motivation

One of the longstanding goals of nuclear physics is to understand how nuclei can be described in terms of Quantum Chromo Dynamics (QCD). Nuclei provide an excellent testing ground for QCD because they are a stable system made up of quarks and gluons bound together by the strong force. However, the quarks and gluons in nuclei are hidden and they seem to be composed of nucleons bound together by exchanging mesons. The primary evidence for nuclear QCD effects comes from the EMC Effect, the ratio of the ratio of the per-nucleon DIS cross section in nucleus A relative to deuterium. This ratio is typically about 1 at $x = Q^2/2m\nu \approx 0.3$ and decreases linearly (in symmetric nuclei) to a minimum around $x \approx 0.7$ [1–3]. This ratio cannot be described by purely nucleonic effects.

The EMC effect has been the object of sustained experimental and theoretical interest with over 1000 papers written on the subject. There is no generally accepted explanation of the EMC effect. However, a recent set of papers showed the remarkably close relationship between the size of the EMC effect in a nucleus and the probability that a nucleon in that nucleus belongs to an NN short-range correlated (SRC) pair [3–5] and showed that the EMC effect can be described by a universal modification of the structure of nucleons in SRC pairs [6]. Current experiments at JLab will test this by measuring the change in the bound-nucleon structure function in deuterium as a function of nucleon momentum [7].

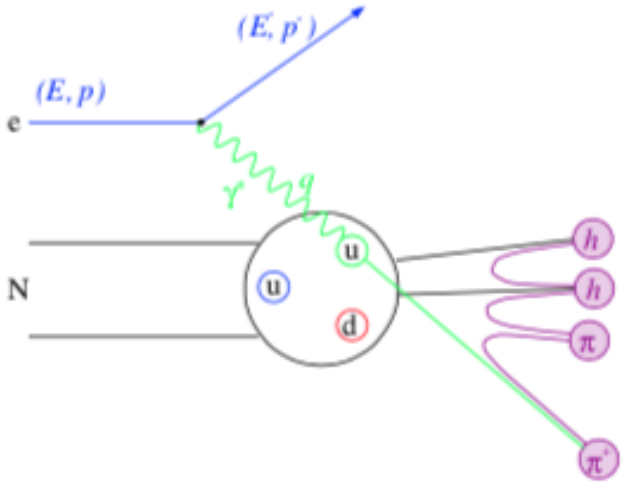

Figure 1: Diagram of semi-inclusive pion production from the nucleon. In this picture, the observed hadron (in this case the π^+) serves as a tag of the flavor of the struck (up) quark.

A second experimental technique is to use the semi-inclusive DIS reaction as a flavor tag (see Fig. 1) to look for signatures of differences in the EMC effect in the up and down quark distributions in asymmetric nuclei (e.g. gold). It has been used successfully, most notably by the HERMES collaboration [8], to deconvolute the relative contributions of up, down, and sea quarks to the spin of the nucleon. However, one can just as easily employ the power of this technique to probe the unpolarized degrees of freedom rather than polarized parton distributions.

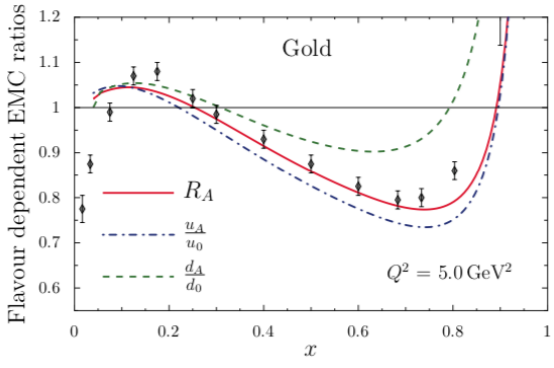

Figure 2: Calculation of the EMC Effect in gold from [9]. Here, gold refers to a calculation for nuclear matter, but assuming the same N/Z as gold. In this model, nuclear quark distributions are modified via interactions with vector and scalar fields in the nucleus. The solid red curve shows the overall modification of the nuclear structure function, F_2. The isospin dependence of the interaction generates a different degree of modification for the up and down quark distributions (shown by the green and blue curves respectively). Nuclear matter "data" points are from [10].

Recent calculations and phenomenological results indicate that the EMC effect will be different in asymmetric nuclei ($N \neq Z$). EMC calculations using the quark-meson coupling (QMC) model of Ref. [11] for "gold" (i.e., for nuclear matter using the same N/Z as gold) predict that the up quark distribution is significantly more modified than the down quark

distribution (see Fig. 2).

Phenomenological results from the EMC-SRC correlation [3–6] show that the EMC effect can be explained by the modification of the structure functions of nucleons in np SRC pairs. This would also give a flavor-dependent EMC effect in asymmetric nuclei. For example, the single proton in ^{3}H can belong to one of two np SRC pairs, but the two neutrons in ^{3}H can each belong to only one. Therefore, the proton in ^{3}H will be more modified than the average of the neutrons. This effect will be reversed in ^{3}He, where the neutron will be more modified than the average of the protons.

We propose to study the flavor dependence of the EMC effect at large x using a new observable, the ratio of charged pion electroproduction in semiinclusive DIS from deuterium, ^{3}He, and ^{3}H targets. The new observables proposed here are the super-ratio of yields $Y(\pi^+)/Y(\pi^-)$ and the ratio of the difference in yields $Y(\pi^+) - Y(\pi^-)$ for the different nuclei. These observables are sensitive to any flavor dependence in modifications to the structure functions inside a nucleus. Thus, by performing a precision measurement of these observables we hope to expose any flavor dependence in the EMC effect and thereby reveal the details of the quark dynamics in nuclei which lead to the modification of the nuclear structure functions.

1.2 Formalism

In general, the cross section for the semiinclusive production of a charged pion can be written as:

$$\frac{d\sigma}{dxdQ^2dz} = \frac{\sum_f e_f^2 q_f(x,Q^2) D_f^h(z,Q^2)}{\sum_f e_f^2 q_f(x,Q^2)} \frac{d\sigma}{dxdQ^2} \tag{1}$$

where $\frac{d\sigma}{dxdQ^2}$ is the inclusive electron scattering cross section, $q_f(x,Q^2)$ is the distribution function for a quark of flavor f and charge e_f, and $D_f^h(z,Q^2)$ is the fragmentation function describing the probability for a quark of flavor f to be found in a hadron off species h carrying a fraction of energy $z = E_h/\nu$ of the energy of the struck quark. Note that we have ignored the azimuthal angle ϕ and the transverse momentum p_t of the outgoing hadron in this expression. We plan to concentrate on hadrons with small p_t in this measurement.

1.2.1 Nuclear Parton Distribution Functions

For a nucleus with Z protons and N neutrons, we define the nuclear PDF (per nucleon) for up and down quarks as:

$$u_A = \frac{Z\tilde{u}_p + N\tilde{u}_n}{A} \tag{2}$$

$$d_A = \frac{Z\tilde{d}_p + N\tilde{d}_n}{A} \tag{3}$$

where $(\tilde{u}_p, \tilde{u}_n)$ and $(\tilde{d}_p, \tilde{d}_n)$ are the up and down quark distributions in the protons and neutrons of the nculeus and the tilde indicates that these might be modified in the nucleus. Assuming isospin symmetry such that

$$u(x) = u_p(x) = d_n(x) \tag{4}$$

$$d(x) = d_p(x) = u_n(x) \tag{5}$$

then we can write:

$$u_A = \frac{Z\tilde{u} + N\tilde{d}}{A} \quad (6)$$

$$d_A = \frac{Z\tilde{d} + N\tilde{u}}{A} \quad (7)$$

and similarly for the anti-quarks.

1.2.2 Flavor Dependence of the EMC Effect

We can then write the per-nucleon semi-inclusive charged pion yield as:

$$Y_A^{\pi^+}/A \propto \frac{4}{9}u_A(x)D_A^+(z) + \frac{1}{9}d_A(x)D_A^-(z) + \frac{1}{9}\bar{d}_A(x)D_A^+(z) + \frac{4}{9}\bar{u}_A(x)D_A^-(z) \quad (8)$$

$$Y_A^{\pi^-}/A \propto \frac{4}{9}u_A(x)D_A^-(z) + \frac{1}{9}d_A(x)D_A^+(z) + \frac{1}{9}\bar{d}_A(x)D_A^-(z) + \frac{4}{9}\bar{u}_A(x)D_A^+(z) \quad (9)$$

where the subscript A on the fragmentation function indicates that they may also be modified in the nucleus. The D^+ and D^- refer to the favored and unfavored fragmentation functions:

$$D^+ = D_u^{\pi^+} = D_{\bar{d}}^{\pi^+} = D_d^{\pi^-} = D_{\bar{u}}^{\pi^-} \quad (10)$$

$$D^- = D_d^{\pi^+} = D_{\bar{u}}^{\pi^+} = D_u^{\pi^-} = D_{\bar{d}}^{\pi^-} \quad (11)$$

and we have ignored strange quark degrees of freedom and and Q^2 dependence for simplicity.

1.2.3 Experimental Observables

We can look at the sums, differences and ratios of the π^+ and π^- yields for the different nuclei. The sum of the $\pi^\pm$ yields should give us back the original EMC effect:

$$\frac{Y(\pi^+ + \pi^-)_A}{Y(\pi^+ + \pi^-)_d} = \frac{4[u_A(x) + \bar{u}_A(x)] + [d_A(x) + \bar{d}_A(x)]}{5[u(x) + \bar{u}(x) + d(x) + \bar{d}(x)]} \times \frac{D_A^+(z) + D_A^-(z)}{D^+(z) + D^-(z)} \quad (12)$$

(with obvious extension to the ^{3}He^{3}H ratio) assuming, for simplicity, no medium modification in deuterium.

Similarly, the ratio of the difference of the yields for ^{3}He or ^{3}H to deuterium is:

$$\frac{Y(\pi^+ - \pi^-)_A}{Y(\pi^+ - \pi^-)_d} = \frac{4[u_A(x) - \bar{u}_A(x)] - [d_A(x) - \bar{d}_A(x)]}{3[u_v(x) + d_v(x)]} \times \frac{D_A^+(z) - D_A^-(z)}{D^+(z) - D^-(z)} \quad (13)$$

where we assumed that $u = u_v + \bar{u}$. The ^{3}He/^{3}H ratio is:

$$\frac{Y(\pi^+ - \pi^-)_{^3\mathrm{He}}}{Y(\pi^+ - \pi^-)_{^3\mathrm{H}}} = \frac{4[u_{^3\mathrm{He}}(x) - \bar{u}_{^3\mathrm{He}}(x)] - [d_{^3\mathrm{He}}(x) - \bar{d}_{^3\mathrm{He}}(x)]}{4[u_{^3\mathrm{H}}(x) - \bar{u}_{^3\mathrm{H}}(x)] - [d_{^3\mathrm{H}}(x) - \bar{d}_{^3\mathrm{H}}(x)]} \times \frac{D_{^3\mathrm{He}}^+(z) - D_{^3\mathrm{He}}^-(z)}{D_{^3\mathrm{H}}^+(z) - D_{^3\mathrm{H}}^-(z)} \quad (14)$$

Lastly we can also extract the π^+/π^- ratio for each nucleus

$$Y_A\left(\frac{\pi^+}{\pi^-}\right) = \frac{[4u_A(x) + \bar{d}_A(x)]D_A^+(z) + [d_A(x) + 4\bar{u}_A(x)]D_A^-(z)}{[4u_A(x) + \bar{d}_A(x)]D_A^-(z) + [d_A(x) + 4\bar{u}_A(x)]D_A^+(z)} \quad (15)$$

and the obvious double ratios.

1.3 Experimental Details

We will use a 10.6 GeV beam (or what ever maximum energy is available when the experiment runs) incident on identical d, ^{3}He, and ^{3}H target cells, detecting the scattered electron and the ejected pions in the CLAS12 forward detector. The target cells will probably be very similar to the successful Hall A d, ^{3}H, and ^{3}He target cells (200 PSI, 12.7 mm diameter, 25 cm long). The large acceptance of CLAS12 will give us a wide acceptance in the important experimental variables of Q^2, x, z and full coverage for small to moderate values of $p_\perp$, the perpendicular momentum of the outgoing pion. We will use the CLAS12 vertex resolution to eliminate events scattering from the target walls. We will only consider pions detected in the common kinematical region where the pi^+ and π^- experimental acceptances are identical.

Because CLAS12 is limited to a luminosity of about 10^{35} cm^{-2}s^{-1}, target heating will be minimal. We anticipate that the tritium target thickness will be the same as the Hall-A tritium target cell with 250 μm aluminum entrance and exit windows and a tritium areal density of 85 mg/cm^2.

1.4 Expected Results

We calculated the various expected ratios of π^+ and π^- yields for three cases, flavor-independent modification of quark distributions, the up quark distribution (but not the down) is modified, and the down quark distribution (but not the up) is modified. The calculations shown here were all performed at $z = 0.5$. The large CLAS12 acceptance will let us measure the z-dependence of the yield ratios over a wide kinematic range.

We used the unpolarized EMC parametrization from the SLAC E139 paper [12] (which describes the Hall C 3He data reasonably well [13]). We used cteq5 for the quark PDFs [14] and a parametrization for the fragmentation functions from e^+e^- data with input from HERMES [15] (which also describes the Hall C SIDIS data pretty well).

The ratios of ^{3}He and ^{3}H to deuterium (see Fig. 3 should be able to differentiate between scenarios where d-quark modification explains the EMC effect and where u-quark or both quarks explain the EMC effect. The ratio of ^{3}He/^{3}H (see Fig. 4a) is not sensitive to these models of flavor-dependence. However, in the EMC-SRC model we expect the protons in ^{3}H and the neutrons in ^{3}He to be more modified, we would expect a significant effect in this ratio for this model.

We do expect to see a much larger difference when we look at the difference in π^+ yields in ^{3}He and ^{3}H divided by the difference in the π^- yields (see Fig. 4b). Again, in the phenomenological EMC-SRC model, we expect that the π^+ yield from ^{3}H and the π^- yield from ^{3}He will be more modified than the complementary channels.

2 Deuteron Knockout

Recent measurements of double-polarization asymmetries in proton and deuteron knockout from ^{3}He [17, 18] have revealed deficiencies in our theoretical understanding of this paradigmatic three-body nuclear system. However, due to the large cancellations of two-body and three-body contributions, as well as the complexity of the Faddeev calculations

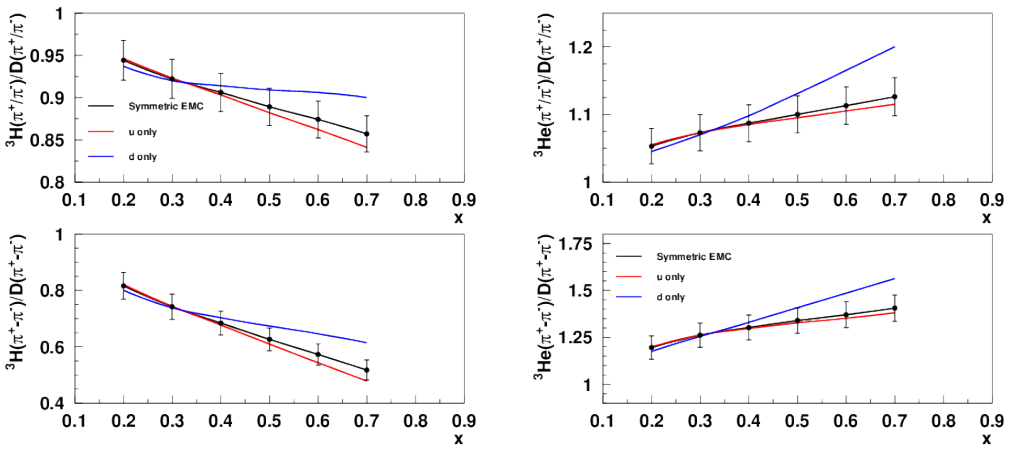

Figure 3: Calculation of the yield ratios of ^{3}H/d and ^{3}He/d using Eqs. 12–15 at $z = 0.5$. The error bars are shown for 2% uncertainty. See text for details.

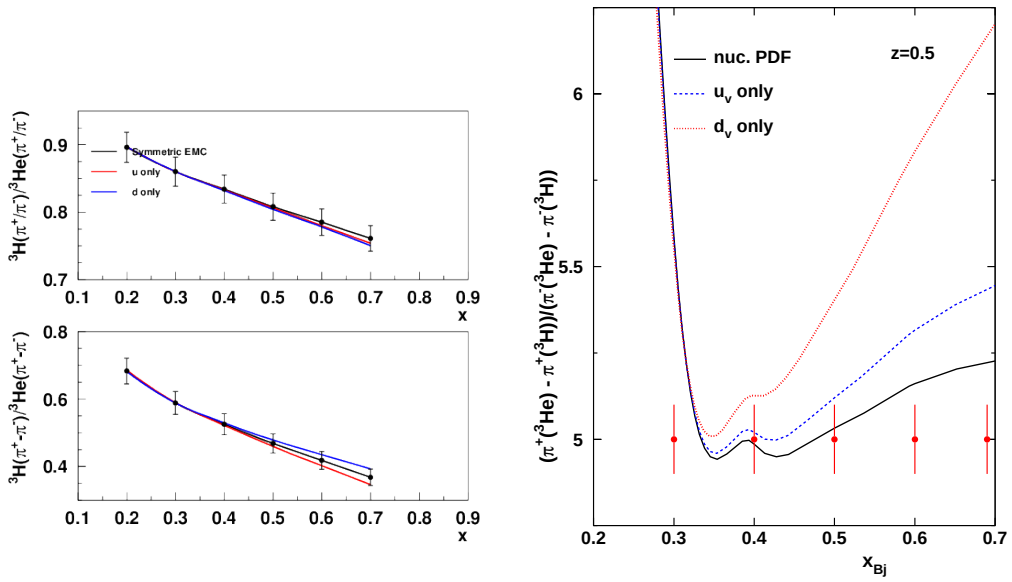

Figure 4: (left) Calculation of the yield ratios of ^{3}He/^{3}H using Eqs. 12–15. (right) The difference in the π^+ yields in ^{3}He and ^{3}H divided by the difference in the π^- yields. The calculations were done at at $z = 0.5$. The error bars are shown for 2% uncertainty. See text for details.

that the data have been compared to, it is extremely challenging to pin-point the exact cause of the failure of what are understood to be nuclear physics' best models.

We propose a systematic and comprehensive study of the effects of adding a nucleon to a nucleus. Specifically, we will make precise measurements of the elastic process $^2\mathrm{H}(e,e'd)$ and compare it to the $^3\mathrm{He}(e,e'd)p$ and $^3\mathrm{H}(e,e'd)n$ reactions over a range of Q^2 and p_{miss} to provide high precision data on how the addition of a nucleon maps to a modification of the knock-out process. Measurements in such broad kinematic ranges will be possible by exploiting the high luminosity of CEBAF, combined with the large acceptance of CLAS12, and the Jefferson Labs unique tritium target.

This could run in parallel with a possible two- or three-pass short range correlations measurement.

3 Tritium Target

We plan to use a special tritum target system for the ^{3}H measurements. Preliminary work by David Meekins indicates that this tritium target system is feasible in Hall B. We will use identical sealed-cell targets for the d and ^{3}He targets. We anticipate (based on estimates of changing target systems for the approved E12-17-006 $e4\nu$ experiment) that it will take two to three days to change target cells.

A tritium target system is required for the proposed measurements. While a detailed conceptual design is not presented here, we propose that such a system should build on the success and lessons learned from the Hall A tritium target which is described in detail in the Hall A Tritium Target Report. The Hall A system relied on a series of engineering and administrative controls to provide three layers of tritium confinement/containment during all phases of installation, operation, and transportation. An exception where only two layers were practical was allowed for brief periods during installation and removal of the cell where the scattering chamber was reconfigured to or from beam operations. A summary of the three layers of containment/confinement are shown in the table below for each operational condition.

Configuration	Layer 1	Layer 2	Layer 3
Installation/Removal	Cell	Handling Hut and Chamber	Hall B
Storage	Cell	Inner Containment Vessel	Outer Containment Vessel
Beam Operations	Cell	Scattering Chamber	Hall B

Note that during beam operations, and Installation/Removal, the Hall must be considered as part of the confinement system. The exhaust system and access controls are designed to ensure that the Hall can indeed be considered one of the layers of confinement. Additionally, any Hall B tritium target is expected to incorporate the same major components as the Hall A system which are listed below.

- Target Cell
- Exhaust system including stack
- Containment/confinement system including the scattering chamber and Hall A.
- Access controls

- Cryogenic cooling system

Because the Hall A target and the proposed Hall B target are very similar, the budget for each system is also expected to be similar. Some expenses that were incurred in the Hall A project, such as the tritium exposure study of aluminum 7075 will not have to be repeated however. The following sections provide a brief description of the major components of the proposed Hall B tritium target.

3.1 Target Cell

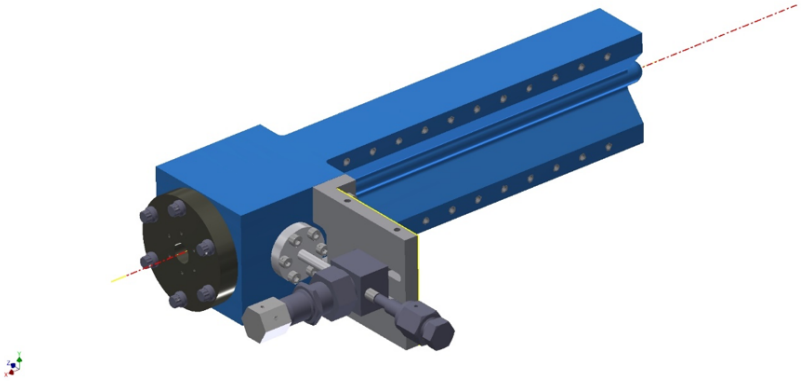

Figure 5: Hall A Tritium target cell. The electron beam is shown as the dashed line and impinges from left to right.

The Hall A tritium target cell is shown in Figure 5. The cell main body incorporated thin sections on the right and left sides of the cell to accommodate the acceptances of the HRSleft/right spectrometers. The thick sections on the top and bottom of the cell allowed heat generated by the beam in the cell exit to be conducted to the cooled heat sink. The proposed cell for the Hall B target requires azimuthal symmetry to accommodate the acceptance of CLAS12. This does not present an issue with regard to beam heating because the production current for the Hall B experiments is expected to be 0.4% of the Hall A production current of $22.5\mu A$. This also greatly simplifies the design of the target cell making it much easier to fabricate. The target cell is expected to be roughly 12.7 mm in diameter and 25 cm long with a fill pressure of about 200 psi. Thus the total amount of tritium would be about 1100 Ci.

3.2 Scattering Chamber and Vacuum System

A large scattering chamber was employed for the Hall A tritium target system. The chamber provided one layer of tritium confinement. The vacuum in the chamber and downstream beam line was maintained by a series of mechanical and turbo pumps. The exhaust of these pumps was directed to a separate 2 inch exhaust line attached to the stack. The chamber was also isolated from the upstream beam line via a 0.2 mm thick beryllium window. A similar system must also be employed in Hall B. Here, the chamber volume must be such that should the tritium cell fail, the scattering chamber will contain all of the tritium gas released and still maintain a sub-atmospheric pressure so that the vacuum pumps can stack the released tritium. The expected operational loss of tritium through the cell walls is about

1 Ci per year due mostly to permeation through the thin cell wall. This is similar to the loss observed in Hall A during operations. This loss although small is collected by the pumping system and stacked through a smaller 2 inch stack (see below) which is purged with air.

3.3 Exhaust System and Stack

A dedicated exhaust system and stack was constructed to remove tritium from Hall A should both the cell and scattering chamber fail. A similar system will be required for Hall B. The exhaust stack must be at least 20m above grade at the site boundary. This ensures that an unlikely tritium release will not cause an undue exposure to the public. The exhaust system can be driven by a fan which pulls air through Hall B into the stack via one of the smoke removal ports. Thus, the exhaust system serves two purposes: tritium removal and smoke removal. Custom ductwork will also be required for proper ventilation of a tritium cell transfer hut which is required for installation and removal operations. This system must also stack the exhaust from the vacuum pumps connected to the scattering chamber and downstream beam line.

3.4 Cryogenic Cooling System

The tritium cell in Hall A was cooled to maintain a temperature of less than 150K in the metallic volume of the cell. This was a design requirement based on previous studies of hydrogen embrittlement in aluminum with an impinging electron beam. In Hall A, the cooling system was supplied by 15K helium from the ESR. For practical reasons, a dedicated cooling system (similar to that of the Hall D cryogenic target) should be used for a Hall B target. Note that the heat load from the beam in the proposed Hall B system is considerably less than in it was in Hall A. A stand alone cryo-cooling system is also expected to improve operational reliability and simplify the design of the system.

3.5 Transportation and Storage

The Hall A Tritium Target cell was filled at Savannah River Site and shipped to Jefferson Lab in the Bulk Tritium Shipping Package (BTSP) as a miscellaneous tritium vesssel (MTV). The same mechanism is expected to be employed for filling and shipping a similar cell for the Hall B target. An expert team from SRS traveled to Jefferson Lab to assist in the unpackaging and packaging of the cell to and from the BTSP. A set of thick shipping covers will be required to protect the cell during handling.

The storage system employed in Hall A can also be used in Hall B. This system allowed the target cell to be removed from the beam line for longer term storage (up to a few months) during accelerator down periods. It also simplifies packaging and unpackaging operations associated with shipment of the cell.

3.6 Tritium Target Conclusion

We conclude that a tritium target similar to the system developed for use in Hall A could be similarly employed in Hall B. While an exhaust system would need to be developed, there are many other aspects of the proposed Hall B system that would make the design

more simple. The proposed target cell would be installed on a dedicated insertion cart for the duration of the tritium run. Therefore, no motion system is required. Further, with the use of a dedicated cryo-cooler and lower beam current the cell and heat sink design are also simplified. A release, in a controlled fashion through the stack or through the truck ramp, of the full load of tritium contained in the cell is not expected to pose a significant to personnel on site or to the public.

References

[1] D. Geesaman, K. Saito, and A. Thomas, "The Nuclear EMC Effect," *Ann. Rev. Nucl. and Part. Sci.*, vol. 45, p. 337, 1995.

[2] P. R. Norton *Rep. Prog. Phys.*, vol. 66, p. 1253, 2003.

[3] O. Hen, G. A. Miller, E. Piasetzky, and L. B. Weinstein, "Nucleon-Nucleon Correlations, Short-lived Excitations, and the Quarks Within," *Rev. Mod. Phys.*, vol. 89, no. 4, p. 045002, 2017.

[4] L. B. Weinstein, E. Piasetzky, D. W. Higinbotham, J. Gomez, O. Hen, and R. Shneor, "Short range correlations and the emc effect," *Phys. Rev. Lett.*, vol. 106, p. 052301, Feb 2011.

[5] O. Hen, E. Piasetzky, and L. B. Weinstein, "New data strengthen the connection between short range correlations and the emc effect," *Phys. Rev. C*, vol. 85, p. 047301, Apr 2012.

[6] B. Schmookler *et al.*, "Modified structure of protons and neutrons in correlated pairs," *Nature*, vol. 566, no. 7744, pp. 354–358, 2019.

[7] O. Hen *et al.* Jefferson Lab experiments E12-11-107 and E12-11-003A.

[8] A. Airapetian *et al.*, "Quark helicity distributions in the nucleon for up, down, and strange quarks from semi-inclusive deep-inelastic scattering," *Phys. Rev. D*, vol. 71, p. 012003, Jan 2005.

[9] I. Cloet, "private communication."

[10] I. Sick and D. Day, "The emc effect of nuclear matter," *Physics Letters B*, vol. 274, no. 1, pp. 16 – 20, 1992.

[11] I. C. Cloet, W. Bentz, and A. W. Thomas, "EMC and polarized EMC effects in nuclei," *Phys. Lett.*, vol. B642, pp. 210–217, 2006.

[12] J. Gomez *et al.*, "Measurement of the a dependence of deep-inelastic electron scattering," *Phys. Rev. D*, vol. 49, p. 4348, 1994.

[13] J. Seely *et al.*, "New measurements of the european muon collaboration effect in very light nuclei," *Phys. Rev. Lett.*, vol. 103, p. 202301, 2009.

[14] H. Lai *et al. Eur. Phys. J. C*, vol. 12, p. 375, 2000.

[15] J. Binnewies, B. A. Kniehl, and G. Kramer, "Pion and kaon production in e^+e^- and ep collisions at next-to-leading order," *Phys. Rev. D*, vol. 52, pp. 4947–4960, Nov 1995.

[16] L. S. Myers, D. W. Higinbotham, and J. R. Arrington, "E12-14-009: Ratio of the electric form factor in the mirror nuclei 3He and 3H," 2014.

[17] M. Mihovilovic *et al.*, "Measurement of double-polarization asymmetries in the quasi-elastic $^3\vec{\mathrm{He}}(\vec{\mathrm{e}},\mathrm{e}'\mathrm{p})$ process," *Phys. Lett. B*, vol. 788, pp. 117–121, 2019.

[18] M. Mihovilovic *et al.*, "Measurement of double-polarization asymmetries in the quasielastic $^3\vec{\mathrm{He}}(\vec{\mathrm{e}},\mathrm{e}'\mathrm{d})$ process," *Phys. Rev. Lett.*, vol. 113, no. 23, p. 232505, 2014.